Possible Fano resonance for high-T_c multi-gap superconductivity in p-Terphenyl doped by K at the Lifshitz transition

Maria Vittoria Mazziotti[1] , Antonio Valletta[2] , Gaetano Campi[3] , Davide Innocenti[4] , Andrea Perali[5] and Antonio Bianconi[1,3,6,7]

[1] *RICMASS, Rome International Center for Materials Science Superstripes, Via dei Sabelli 119A, 00185 Rome, Italy*
[2] *Institute for Microelectronics and Microsystems, IMM, Consiglio Nazionale delle Ricerche CNR, Via del Fosso del Cavaliere 100, 00133 Roma, Italy*
[3] *Institute of Crystallography, IC, Consiglio Nazionale delle Ricerche CNR, via Salaria, Km 29.300, 00015 Monterotondo Roma, Italy*
[4] *Department of Chemistry, University of Liverpool, Liverpool, L69 7ZD, UK*
[5] *School of Pharmacy, Physics Unit, University of Camerino, Camerino, Italy*
[6] *National Research Nuclear University MEPhI (Moscow Engineering Physics Institute) 115409 Moscow Kashirskoe shosse 31 Russia*
[7] *Latvian Academy of Sciences Akad?mijas Laukums 1, R?ga, LV-1050 Latvia*

PACS 74.70.Kn – noncuprate superconductors
PACS 74.20.-z – Theories and models of superconducting state
PACS 74.10.+v – Occurrence, potential candidates

Abstract –Recent experiments have reported the emergence of high temperature superconductivity with critical temperature T_c between 43K and 123K in a potassium doped aromatic hydrocarbon para-Terphenyl or p-Terphenyl. This achievement provides the record for the highest T_c in an organic superconductor overcoming the previous record of T_c=38 K in Cs_3C_{60} fulleride. Here we propose that the driving mechanism is the quantum resonance between superconducting gaps near a Lifshitz transition which belongs to the class of Fano resonances called shape resonances. For the case of p-Terphenyl our numerical solutions of the multi gap equation shows that high T_c is driven by tuning the chemical potential by K doping and it appears only in a narrow energy range near a Lifshitz transition. At the maximum critical temperature, T_c=123K, the condensate in the appearing new small Fermi surface pocket is in the BCS-BEC crossover while the T_c drops below 0.3 K where it is in the BEC regime. Finally we predict the experimental results which can support or falsify our proposed mechanism: a) the variation of the isotope coefficient as a function of the critical temperature and b) the variation of the gaps and their ratios $2\Delta/T_c$ as a function of T_c.

Introduction. – Recently high temperature superconductivity with T_c in the range of 43-123 K has been reported following different growth procedures in a potassium doped aromatic hydrocarbon p-Terphenyl [1–3]. The superconducting crystalline phase is expected to be $K_3C_{18}H_{14}$. Superconducting pairing with a large 15 meV gap opening at about 60K was confirmed on a K-doped surface of a p-Terphenyl single crystal [4]. Para-Terphenyl, a linear molecule made of a chain of 3 benzene rings, and its derivatives are aromatic biological molecules present in edible mushrooms [5]. Pharmaceutical research is in progress for their use as immunosuppressive, anti-inflammatory and anti-tumor agents, and it also has technological applications as laser dye, sunscreen lotion and in photon detectors. If these results will be confirmed, K_x p-Terphenyl provides today the record for the highest critical temperature in carbon based materials and larger than in many cuprates oxides and in many iron based superconductors. The search for macroscopic quantum coherence at high temperature in organics and organometallics has been a long standing search for the holy grail of room temperature superconductors. Superconductivity in graphite

intercalation compounds has been an active topic for several decades, but T_c ranges only up to 11.5 K for CaC_6 [6]. The highest critical temperature T_c=38 K in doped fullerides A_3C_{60} $A = K, Rb, Cs$ has been found in Cs_3C_{60} with A15 structure by application of 7 Kbar hydrostatic pressure [7]. This system provides a complex phase of condensed matter where structural polymorphism controls both magnetic and superconducting properties [8] and shows a fluctuating microscopic heterogeneity made of the coexistence of both localized Jahn-Teller active and itinerant electrons [9]. Recently the material research for high temperature superconductors was oriented toward metal-intercalated aromatic hydrocarbons by the discovery of superconductivity with T_c=18K by doping potassium into picene ($C_{22}H_{14}$) [10,11]. Picene is a hydrocarbon molecule made of five benzene rings condensed in an armchair manner. Looking for high T_c in alkali-metals or alkali-earth-metals doped polycyclic-aromatic-hydrocarbons (PAHs), the previous record T_c=33 K was held by in K_x 1,2:8,9-dibenzopentacene ($C_{30}H_{18}$) [12]. The recent indications for T_c=123K in p-Terphenyl open a new roadmap for the search of higher critical temperatures in the large family of doped metal-organic compounds, with the hope to overcome the highest superconducting critical temperature known so far, T_c=203K in pressurized H_3S [13,14]. There is today high interest on understanding both the quantum mechanism beyond the emergence of T_c=123K in p-Terphenyl and the relation between the nanostructure and quantum functionality in organics. This is needed to develop novel *quantum plastics* materials, taking advantage that conducting polymers can be prepared in a large variety of polymeric heterostructures at atomic limit [15–17] and possess the combination of easy processability, light weight, and durability. Using density functional theory and Eliashberg's theory of superconductivity in the single band approximation the superconducting critical temperature has been predicted to be in the range $3 < T_c < 8$ K in K_3 picene [18] and around 6.2 K in $K_2C_6H_6$ moreover, it was argued that all hydrocarbons should show T_c in a similar temperature range of $3 < T_c < 7$K [19]. A hot topic today is the search for superconductivity in the extreme high pressure phases of benzene [20–22]. Therefore unconventional pairing mechanisms were invoked for high T_c in doped p-Terphenyl: a) the Bose-Einstein Condensation (BEC) of preformed bipolarons [1–3]; b) the Resonating Valence Bond (RVB) theory in a scenario with two coexisting doped Mott insulators [23] c) the so called $s_{+/-}$ pairing mechanism mediated by a repulsive interaction in a scenario with two strongly correlated bands forming two similar Fermi surfaces connected by a nesting vector [24].

Here we propose the mechanism for T_c amplification driven by Fano resonance [25, 26] in a multigap superconductor between different gaps occurring where the chemical potential is tuned at a electronic topological Lifshitz transition [27]. In this regime the configuration interaction between the pairing scattering channels in the (n-1)-th bands with high Fermi energy $E_{F(n-1)}$ in the BCS approximation and the n-th pairing scattering channel in the new appearing n-th small Fermi surface with a low Fermi energy E_{Fn}) can give a resonance in the superconducting gaps, called shape resonance [28,29] like in nuclear physics and molecular physics [30] or Feshbach resonance as in the jargon of ultracold gases [31]. The Fano resonance give high T_c domes around Lifshitz transitions in the energy range of E_{Fn} of the order of the energy of the pairing cut-off and the n-th condensate is in the BCS-BEC crossover [32, 33].

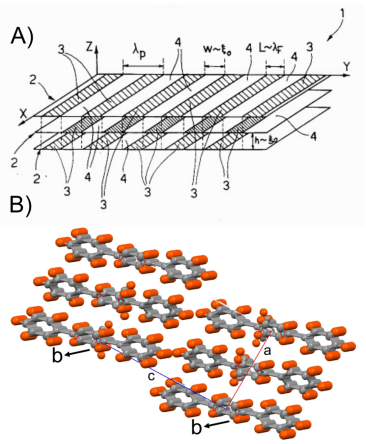

Fig. 1: A) Drawing of the heterostructure at atomic limit made of nanoscale stripes which promotes shape resonances according to Ref. [26]. The stripes run along the x direction of the xy planes which are separated along the z direction. B) The p-Terphenyl crystal structure P21/a (CCDC reference No. 847173) appears as a practical realization of the superlattice of stripes shown in panel (A) made of p-Terphenyl striped units of atomic thickness. In the P21/a structure the **b**, **c** and **a** axis correspond to the x, y and z axis in the schematic drawing in panel (A). The p-Terphenyl stripes run along the **b** direction and are well separated by the neighbor stripe along the **c**-axis and the **a**-axis directions

The configuration interaction between pairing channels is determined by the symmetry and interference between the wavefunctions of electron pairs at the coexisting multiple Fermi surfaces therefore the nanoscale material architecture plays a central role. In ref [25, 26] particular material architectures made by heterostructures on the atomic scale which could give high-T_c superconductors have been disclosed. Panel (A) in Fig. 1 shows one of these heterostructures at atomic limit: a superlattice of stripes. In this case the material is made of nanoscale modules, metallic stripes of atomic thickness, as for example metallic graphene or phosphorene nanoribbons assembled in a superlattice of stripes separated by potential barriers from neighbor stripes in the same plane or in the neighbor plane. The size of the nanoscale units or modules and the superlattice period λ_p is required to be in the nanoscale. In fact, in order to attain the highest T_c, it is necessary to tune the Fano resonance with the wavelength of the electrons at the Fermi level in the n-th band λ_{Fn}

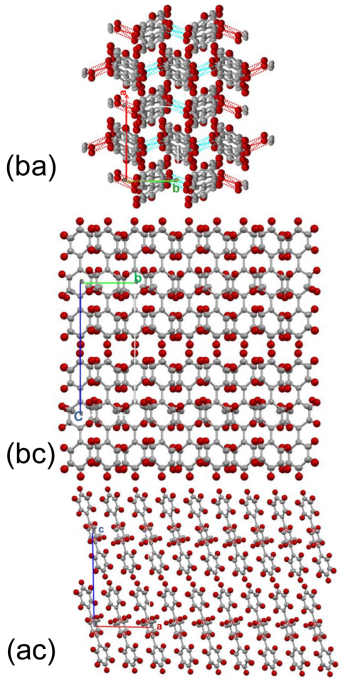

Fig. 2: Three different projections of the p-Terphenyl crystal structure, monoclinic space group P21/a, with axis **a**=0.81 nm, **b**=0.56 nm, **c**=1.36 nm and β=92°. The **bc** projection shows two parallel p-Terphenyl stripes, made of linear p-Terphenyl molecules, running in the **b** axis direction, the packing of these stripes form a superlattice of stripes with a period of 1.36 nm in the **c** direction. The upper **ba** projection shows the lateral view of the p-Terphenyl stripes. The lower **ac** projection shows the packing of stripes, running in the **b** axis direction, perpendicular to the page well separated by neighbor stripe forming a superlattice of stripes with period of 0.81 nm in the **a** axis direction.

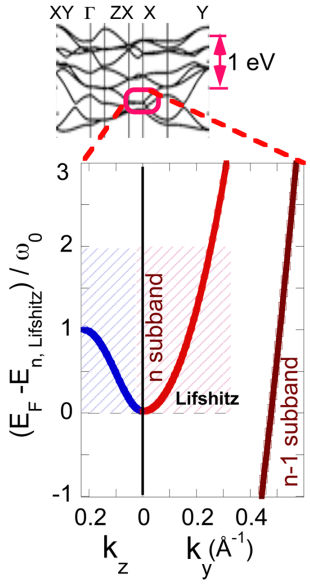

Fig. 3: Panel (A) shows the Brillouin zone (BZ) representation of the conduction band of the p-Terphenyl from Ref. [35]. The 2 eV wide conduction band is made by a bundle of many bands showing a large dispersion in the Y direction, the direction of the p-Terphenyl stripes, and flat dispersions in the ZX directions, orthogonal to the stripes direction. The red circle indicates a narrow energy range of about 600 meV around the band edge of the n-th electronic band which shows the narrow energy dispersion in the XZ direction and wide dispersion in the Y direction which coexist with other (n-1)-th dispersing bands. Panel (B) shows the dispersion of the electronic bands obtained by solution of the Schroedinger equation for a superlattice of stripes with period 1.4 nm, separated by a potential barrier, determined by the hopping energy between stripes, in the transversal direction is such that the transversal energy dispersion in the periodic potential is 145 meV the same as the assumed energy cut off for the pairing ω_0=145 meV. The narrow energy range of the dome of high T_c is only of the order of $4\omega_0$=580 meV, where the Fano resonance near the Lifshitz transition is in action.

in the range of λ_p. The crystalline structure of undoped p-Terphenyl [34] with a monoclinic space group P21/a is shown in Panel (B) of Fig. 1 where gray dots are carbon atoms and red dots are hydrogen atoms, can be described as a packing of parallel p-Terphenyl nanoribbons or stripes of about 1.4 nm width running in the **b**-axis direction indicated by the black arrows. The figure shows the similarity of the arrangements of the p-Terphenyl nanoscale stripes with the schematic drawing of the superlattice of stripes shown in panel (A) of Fig. 1 from ref [26]. The projections in the **ac**, **bc** and **ba** crystal planes are shown in Fig. 2. Two parallel stripes are clearly seen in the **bc** projection. The **ba** projection in Fig. 2 shows a variable torsion angle (up to 14 degrees) of the middle ring relative with the two lateral ones. While the $H-H$ bond is 0.32 nm between the lateral rings of the neighbor molecules very short $H-H$ intermolecular bonds (dashed lines connecting neighbor molecules in the stripe in the **b** direction) are established for the central benzene ring, as short as 0.22 nm, like the shortest values observed in the high pressure phases of benzene [20, 21]. The stripes are not connected with the neighbor stripes also in the a-axis direction indicating the quasi one dimensional electronic structure of the stripes.

The electronic structure of p-Terphenyl [24, 35, 36] confirms the presence of one dimensional electronic states in the conduction band. A portion of the electronic structure of the conduction band [35] is shown in the upper part of Fig. 3. The band structure, upper panel of Fig. 3, displays in a clear way a strong anisotropic character in the wave-vector space. Indeed, in the irreducible representation of the band structure reported in the upper part of Fig. 3 [24,35,36] shows two directions in the Brillouin zone for which the band dispersions are very narrow. A narrow bandwidth of the order of hundred meV, indicates that large potential barriers have to be penetrated by the electrons to tunnel from one p-Terphenyl stripe to its neighbor stripe. Interestingly and relevantly for this work, all the

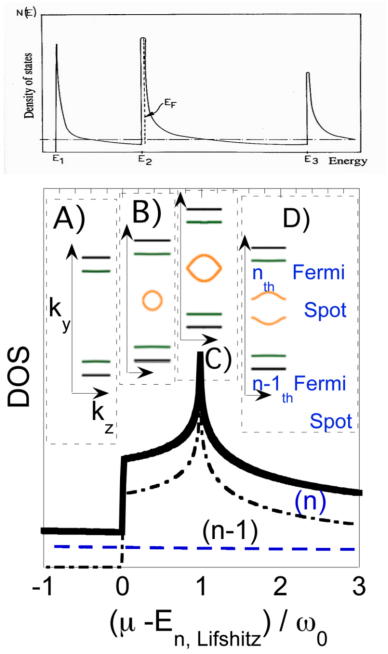

Fig. 4: The density of states (DOS) for the superlattice of stripes which simulate the DOS at the Van Hove singularity associated with a 1st Lifshitz transition for the appearing of a new circular Fermi surface and a 2nd 2D-1D topological Lifshitz transition. Panels (A), (B), (C) and (D) show the evolution of the Fermi surfaces arcs and pockets as the chemical potential is increased through the Lifshitz transition, in the energy range of $4\omega_0$. When the chemical potential moves from below to above the bottom of the n-th band, i.e., at the first Lifshitz transition for the appearing of a new Fermi surface, the pocket with 2D character appears in panel (B) Continuing to increase the chemical potential, at the second Lifshitz transition, at the Van Hove singularity, panel (C) , the Fermi surface pocket opens a neck and the new Fermi surface acquires a 1D behavior forming Fermi arcs, panel (D).

bands of the band-bundle due to the different overlapping orbitals of the p-Terphenyl, have this property and are very narrow along these two independent directions, indicating that the potential barrier formed by the crystal structure and by the characteristics of the electronic bonds is felt by all the conduction and valence electrons. In the b-axis direction in the real space, orthogonal to the upper surface of the Brillouin zone the band dispersion is much broader, of the order of 700 meV, pointing toward a quasi-free conduction of the electrons with a moderate effective mass along the b direction. The energy scale of the pairing,145 meV, is taken from the relevant phonons detected at 1171 cm-1, due to a mode of the C-C bond, and/or the mode at 1222 cm-1 of the C-H mode, detected by Raman spectroscopy in metallic K_3 p-terphenyl [1]. We have simulated the band dispersion and the DOS with a periodic potential barrier with 1.4 nm periodicity which reproduces the narrow band dispersion in the transversal direction of the stripes shown in the lower panel of Fig. 3. We have obtained an electronic structure which reproduce the key features observed when the chemical potential is tuned at a band edge in a superlattice of stripes as shown in the upper panel of Fig. 4 showing the drawing of the patent for material design of heterostructures at atomic scale [26]. Once doped by K, the chemical potential will be raised in the conduction band and depending of the doping (and/or misfit strain, pressure, orientational disorder, magnetic field ...) at the n-th band edge giving rise to a complex network of Fermi surfaces, with electron and hole-like small pockets of Fermi surfaces and Fermi arcs. The key point of this work is to predict the superconducting properties of the K-doped p-Terphenyl with numerical calculations through a simplified model of its nanoscale structure getting the key electronic structure near a band edge. The bands and wave-functions are created by using a proper superlattice of stripes, which allow the solution of the Bogoliubov gap equations [37,38] without standard BCS approximations, giving high-T_c superconducting state with multigaps and multi-condensates at different BCS/BEC pairing regimes. The pairing is thought to be driven by an attractive interaction within each Fermi surface, but the non-diagonal interaction between condensates can be either repulsive or attractive. The multicomponent character of the pairing and the geometry of the system will determine shape resonances in the superconducting gaps and T_c, with peculiar features predicted for the isotope effect and the gap to T_c ratios, which can be tested in future experiments, together with the expected anisotropic transport of electrons in doped (or out of equilibrium) single crystals. The presence of high temperature superconducting domes where the chemical potential crosses the Lifshitz transitions has now well confirmed by experiments in iron based superconductors. Here we present the possible scenario of high temperature superconductivity in p-Terphenyl where the chemical potential is driven by potassium doping at a Lifshitz transition. Our model predicts that at the Lifshitz transition the Fermi surface is made of multiple components: circular Fermi surface pockets and Fermi arcs as shown in Fig.4. The superconducting properties have been calculated using the Bianconi-Perali-Valletta (BPV) theory which describes a solution of the Bogoliubov-de-Gennes BdG equations for inhomogeneous superconducting phase. The BPV theory has been used to predict the high T_c in striped cuprates [39–42], proposing the coexistence of Fermi arcs and Fermi pockets, which was confirmed in 2009 [43], and the anomalous isotope coefficient [44,45]. The BPV theory has been applied to diborides [46–48], and iron based superconductors [49–51] where it has been confirmed by recent experiments [52–56]. In these experiments it has been reported compelling evidence that the high T_c domes occur in the proximity of the Lifshitz transitions for the appearing of a new Fermi surface pocket. Recently similar scenarios have been proposed for pressurized sulfur hydrides [57] and in superconducting nanofilms [58] Let us consider a system made of multiple bands with index n. The energy separation be-

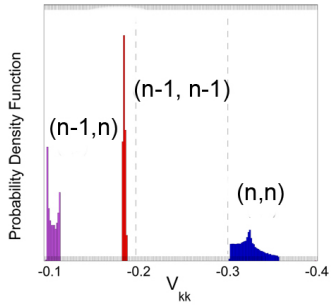

Fig. 5: Matrix elements of the effective pairing interaction for electrons of the (n-1)-th and n-th bands, calculated from the overlap integral of the single-particle wave-functions of the superlattice potential. Matrix elements for the intraband and exchange-pair processes are reported, demonstrating an interesting wave-vector dependence for the two-particle scatterings involving the electrons of the upper n-th band.

tween the chemical potential and the bottom of the n-th band defines the Fermi energy of the n-th band. This formulation was proposed for systems with a band crossing the chemical potential having a steep free electron like dispersion in the x direction and a flat band-like dispersion in the y direction. The wavefunctions of electrons at the Fermi level are calculated using a lattice with quasi-one dimensional lattice potential modulation where the chemical potential is tuned near a Lifshitz transition, like in magnesium diborides, A15, cuprates, iron based superconductors and we propose here for doped p-terphenyl.

The superconducting critical temperature T_c in the BPV theory is obtained by numerical solution of the gaps equation [37,38] considering the simplest case of a two dimensional system [41] of stripes, but the extension to three dimensional system [48] is straightforward. The T_c is determined by solving the following selfconsistent system of equations,

$$\Delta_{n,k_y} = -\frac{1}{2N}\sum_{n',\mathbf{k'}} V^{n,n'}_{\mathbf{k},\mathbf{k'}} \frac{\tanh(\frac{E_{n,k'_y}+\epsilon_{k_x}-\mu}{2T_c})}{E_{n,k'_y}+\epsilon_{k_x}-\mu}\Delta_{n',k'_y}, \qquad (1)$$

where the $E_{n,k_y}+\epsilon_{k_x}$ is the energy dispersion and μ the chemical potential. We consider a superconductor with multiple gaps Δ_{n,k_y} in multiple bands n with flat band-like dispersion in the y direction and steep free-electron-like dispersion in the x direction for a simple model of a two dimensional metal with a one-dimensional superlattice modulation in the y-direction. The self consistent equation for the gaps at $T=0$ where each gap depends on the other gaps is given by

$$\Delta_{n,k_y} = -\frac{1}{2N}\sum_{n',k'_y,k'_x} \frac{V^{n,n'}_{\mathbf{k},\mathbf{k'}}\Delta_{n',k'_y}}{\sqrt{(E_{n',k'_y}+\epsilon_{k'_x}-\mu)^2+\Delta^2_{n',k'_y}}}, \qquad (2)$$

where N is the total number of wave-vectors in the discrete summation and $V^{n,n'}_{\mathbf{k},\mathbf{k'}}$ is the effective pairing interaction

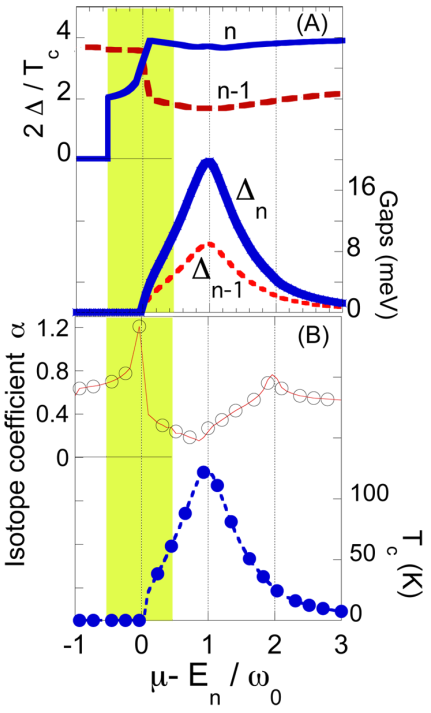

Fig. 6: Results of the BPV theory for the superconducting state properties as a function of the energy distance from the 2D-1D Lifshitz transition. Panel (A). Superconducting gaps at zero temperature which open in the band n and n-1, and gaps to T_c ratios. Panel (B). Superconducting critical temperature and corresponding isotope coefficient. The maximum gaps and T_c are located at the 2D-1D dimensional crossover, with a broad resonance induced by the large value of the phonon energy ω_0=145 meV.

taken in the separable and energy cutoff approximation,

$$V^{n,n'}_{\mathbf{k},\mathbf{k'}} = \widetilde{V}^{n,n'}_{\mathbf{k},\mathbf{k'}}\theta(\omega_0-|E_{n,k_y}+\epsilon_{k_x}-\mu|)\theta(\omega_0-|E_{n',k'_y}+\epsilon_{k'_x}-\mu|). \qquad (3)$$

Here we take account of the interference effects between the single-particle wave functions of the pairing electrons in the different bands, where n and n' are the band indexes, $k_y(k'_y)$ is the superlattice wave-vector and $k_x(k'_x)$ is the component of the wave-vector in the free-electron-like direction of the initial (final) state in the pairing process.

$$\widetilde{V}^{n,n'}_{\mathbf{k},\mathbf{k'}} = -\frac{\lambda_{n,n'}}{N_0}S \times \int_S \psi_{n',-k'_y}(y)\psi_{n,-k_y}(y)\psi_{n,k_y}(y)\psi_{n',k'_y}(y)dxdy, \qquad (4)$$

N_0 is the DOS at the Fermi energy E_F without the lattice modulation, $\lambda_{n,n'}$ is the dimensionless coupling parameter, $S=L_xL_y$ is the surface of the plane and $\psi_{n,k_y}(y)$ are the eigenfunctions in the 1D superlattice. We have used weak coupling intraband coupling constants 0.14 for the (n-1)-th bands, 0.2 for the appearing n-th band and a small 0.1 interband attractive or repulsive exchange interband pairing constant and the distribution of calculated intraband pairing terms (n,n) (n-1,n-1) together with the (n,n-1) interband terms is shown in Fig. 5.

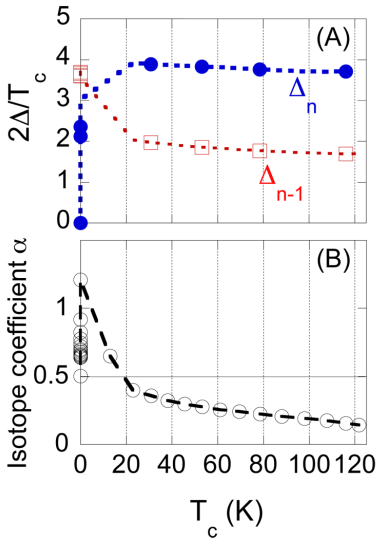

Fig. 7: Superconducting state properties reported as a function of T_c predicted by the BPV theory. Panel (A). Zero temperature superconducting gaps to T_c ratios. Panel (B). Isotope coefficient for the isotope effect on the critical temperature. Different K doping levels, not well under control in the experiments, will correspond to different critical temperatures, which can be used to find the associated superconducting properties in the figure.

The system of equations for the gaps need to be solved iteratively. The anisotropic gaps depend on the band index and on the superlattice wave-vector k_y. According with Leggett [59] the ground-state BCS wave function corresponds to an ensemble of overlapping Cooper pairs at weak coupling (BCS regime) and evolves to molecular (non-overlapping) local pairs with bosonic character in the BEC regime. This approach remains valid also if a particular band is in the BCS-BEC crossover and beyond Migdal approximation because all other bands are in the BCS regime and in the Migdal approximation. In this crossover regime the chemical potential μ results strongly renormalized with respect to the Fermi energy E_{Fn} of the non interacting system. In the case of a Lifshitz transition, as described in this paper, nearly all electrons in the new appearing Fermi surface condense forming a condensate having a BCS-BEC crossover character.

Therefore at any chosen value of the charge density ρ for a number of the occupied bands N_b, the chemical potential in the superconducting phase has to be renormalized by the gap opening solving the following equation:

$$\rho = \frac{1}{L_x L_y} \sum_{n}^{N_b} \sum_{k_x,k_y} \left[1 - \frac{E_{n,k_y} + \epsilon_{k_x} - \mu}{\sqrt{(E_{n,k_y} + \epsilon_{k_x} - \mu)^2 + \Delta^2_{n,k_y}}} \right]. \tag{5}$$

Three distinct regimes of multi-gap superconductivity are obtained as a function of the chemical potential tuned around the 2D-1D Lifshitz transition, as reported in Fig. 6. At the n-th band bottom, when the new Fermi surface pocket starts to appear, there is a coexistence of a BCS-like condensate of the pairs of the (n-1)-th band together with a BEC-like condensate of the pairs of the n-th band, which because of the very low density condense completely in a bosonic liquid. In this regime the critical temperature is extremely low and small variations of the parameters can lead to large variations in the gaps and in the T_c, determining a large peaked value of the isotope coefficient. The peak in the isotope coefficient reported in panel (B) is a finger print of our BPV theory and it signals the strong interplay between the Lifshitz transition at the band bottom and the onset of shape resonant superconductivity. Increasing the chemical potential trough the second Lifshitz transition, the resonant regime of maximum T_c and gaps is obtained. This resonant regime is characterized by an interesting coexistence of BCS-like pair condensate of the (n-1)-th band and BCS-BEC crossover-like pair condensate of the n-th band. In the resonance regime the two gaps differ by a sizable 2.5 factor, the isotope effect gets its smallest values and T_c can reach the high value of 123 K with coupling strengths in the different channels not exceeding 0.3, values still typical of metals, as Nb. The large energy scale of the phonon (145 meV) determines not only a large prefactor for the critical temperature, but also induces a large width of the resonant regimes, making relatively simple to find the right doping levels giving the highest critical temperatures. Finally, for larger chemical potentials, a third regime of conventional two-band superconductivity is reached, with coexistence of two-particles condensates having both BCS-like character, confirmed also by values of the isotope coefficient approaching 0.5 and small values of the gaps typical of weakly-coupled superconductors. The predicted zero temperature superconducting gaps to T_c ratios, panel (A), and the Isotope coefficient as function on the critical temperature, panel (B) are reported in Fig. 7 so that the present theoretical work can be confirmed by direct experiments. This theory does not include superconducting fluctuations. However it should be noticed that in a multigap / multiband system another fundamental phenomenon helps in stabilizing high temperature superconductivity: the screening of the superconducting fluctuations. In fact the multi-band BCS-BEC crossover in a two-band superconductor (one condensate in the BCS regime, the other in the BCS-BEC regime) can determine the optimal condition to allow the screening of the detrimental superconducting fluctuations due to the large stiffness of the BCS-like condensate in the deep band. Finally an arrested or frustrated phase separation is expected to occur at a topological Lifshitz transition [60, 61] as it was observed in cuprates, and diborides [62, 63], diborides [64].

* * *

This work has been supported by superstripes-onlus. Discussions with Gianni Profeta, Augusto Marcelli, Nicola Poccia, Andrea Ienco, Corrado Di Nicola, Fabio Marchetti, Claudio Pettinari are acknowledged.

REFERENCES

[1] Gao Y., Wang R.-S., Wu X.-L., Cheng J., Deng T.-G., Yan X.-W. and Huang, Z.-B, *Acta Physica Sinica*, **65** (2016) 077402.

[2] Wang R.-S., Gao Y., Huang Z.-B. and Chen X.-J., *Arxiv:1703.05804*, **2017** ()

[3] Wang R.-S., Gao Y., Huang Z.-B. and Chen X.-J., *Arxiv:1703.06641*, **2017** ()

[4] Li H., Zhou X., Parham S., Nummy T., Griffith J., Gordon K., Chronister E. L. and Dessau D. S., *Arxiv:1704.04230*, **2017** ()

[5] Liu J.-K., Hu L., Dong Z.-J. and Hu Q., *Chemistry & Biodiversity*, **1** (2004) 601-605.

[6] Weller T. E. et al., *Nature Phys.*, **1** (2005) 39-41

[7] Ganin A. Y., Takabayashi Y., Khimyak Y. Z., *et al.*, *Nature Materials*, **7** (2008) 367-371.

[8] Ganin A. Y., Takabayashi Y., Jeglic P. *et al.*, *Nature*, **466** (2010) 221-225.

[9] Zadik R. H., Takabayashi Y., Klupp G., *et al.*, *Science Advances*, **1** (2015) e1500059.

[10] Mitsuhashi R. *et al.*, *Nature*, **464** (2010) 76-79.

[11] Kubozono, Y., Mitamura, H., Lee, X., et al , *Physical Chemistry Chemical Physics*, **13** (2011) 16476-16493

[12] Xue M., *et al.*, *Scientific Reports*, **2** (2012) 389.

[13] Drozdov P., Eremets M.I.,Troyan I.A., Ksenofontov V. and Shylin S.I., *Nature*, **525** (2015) 73-76

[14] Bianconi A. and Jarlborg T., *EPL (Europhysics Letters)*, **112** (2015) 37001

[15] Faramarzi, *et al.*, *Nature Chemistry* , **4** (2012) 485-490

[16] Malvankar, N. S. *et al.*, *Nature Nanotechnology*, **6** (2011) 573-579

[17] Botta, C., Destri, S., Porzio, W., and Tubino, R., *The Journal of Chemical Physics*, **102** (1995) 1836-1845,

[18] Casula M., Calandra M., Profeta G. and Mauri F., *Physical Review Letters*, **107** (2011) 137006

[19] Zhong G., Chen X.-J. and Lin H.-Q., *arxiv:1501.00240*, **2015** ()

[20] Wen X.-D., Hoffmann, R. and Ashcroft N., *J. Am. Chem. Soc.*, **133** (1993) 9023-9035.

[21] Katrusiak A., Podsiado M. and Budzianowski A., *Crystal Growth & Design* , **10** (2010) 3461-3465.

[22] Hofmann D.W.M. and Kuleshova L.N., *Crystal Growth & Design*, **14** (2014) 3929-3934.

[23] Baskaran G., *Arxiv:1704.0815*, **2017** ()

[24] Fabrizio M., Qin T., Naghavi S. S. and Tosatti E., *arxiv:1705.05066*, **2017** ()

[25] Bianconi A., *Solid State Communications*, **89** (1994) 933.

[26] Bianconi A., *US Patent*, **6,265,019** (2001) priority date Dec 7, 1993.

[27] Volovik G.E., *Low Temperature Physics*, **43** (2017) 47-55.

[28] Bianconi A., *J. Phys.: Conf. Ser.*, **449** (2013) 012002.

[29] Bianconi A., *Journal of Superconductivity*, **18** (2005) 625.

[30] Vittorini-Orgeas A. and Bianconi A., *Supercond. Nov. Magn.*, **22** (2009) 215.

[31] Chin C., Grimm R., Julienne P. and Tiesinga E., *Rev. Mod. Phys.*, **82** (2010) 1225.

[32] Perali A., Pieri P. and Strinati G.C., *Phys. Rev. Lett.*, **93** (2004) 100404.

[33] Guidini A. and Perali A., *Supercond. Sci. Technol.*, **27** (2014) 124002.

[34] Rice A., Tham F. and Chronister E., *Journal of Chemical Crystallography*, **43** (2013) 14-25.

[35] Puschnig P., Heimel G., Weinmeier K., Resel R. and Ambrosch-Draxl C., *High Pressure Research*, **22** (2002) 105-109.

[36] Koller G. *et al.*, *Science*, **317** (2007) 351-355.

[37] Annett J.F., *Superconductivity, Superfluids and Condensates* (Oxford University Press, Oxford) 2004

[38] Svistunov B.V., Babaev E.S. and Prokof'ev N.V., *Superfluid States of Matter* (CRC Press) 2015

[39] Perali A. Bianconi A. Lanzara, A. and Saini N.L., *Solid State Commun.*, **100** (1996) 181.

[40] Valletta A., Bianconi A., Perali A. and Saini N.L., *Zeitschrift fur Physik B Condensed Matter*, **104** (1997) 707.

[41] Bianconi A., Valletta A., Perali A. and Saini N.L., *Physica C: Superconductivity*, **296** (1998) 269 .

[42] Müller K. A. and Bussmann-Holder A. (Editors), *Superconductivity in complex systems, in Structure and Bonding*, Vol. **114** (Berlin, Heidelberg) 2005

[43] Meng J. *et al.*, Liu, G., Zhang, W., Zhao, L., Liu, H., Jia, X., Mu, D., Liu, S., Dong, X., Zhang, J., Lu, W., Wang, G., Zhou, Y., Zhu, Y., Wang, X., Xu, Z., Chen, C., and Zhou, X.J *Nature*, **462** (2009) 335-338.

[44] Perali A., Innocenti D., Valletta A. and Bianconi A., *Supercond. Sci. Technol.*, **25** (2012) 124002

[45] Innocenti D., and Bianconi A., *Supercond. Nov. Magn.*, **26** (2013) 1319-1324.

[46] Bianconi A., Di Castro D., Agrestini S., Campi G., Saini N. L., Saccone A., De Negri S. and Giovannini M., *Journal of Physics: Condensed Matter*, **13** (2001) 7383.

[47] Bussmann-Holder A. and Bianconi A., *Phys. Rev. B* , **67** (2003) 132509.

[48] Innocenti D. *et al.*, *Phys. Rev. B*, **82** (2010) 184528.

[49] Caivano, R. *et al.*, *Supercond. Sci. Technol.*, **22** (2009) 014004.

[50] Innocenti D., Valletta A. and Bianconi A., *Supercond. Nov. Magn.*, **24** (2011) 1137.

[51] Bianconi A., *Nature Physics* , **9** (2013) 536.

[52] Kordyuk A.A. *et al.*, *Supercond. Nov. Magn.*, **26** (2013) 2837.

[53] Kordyuk A.A., *Low Temperature Physics* , **41** (2015) 319-341.

[54] C. Liu *et al.*, *Physical Review B* , **84** (2011) 020509.

[55] Ideta S. *et al.* , *Phys. Rev. Lett.*, **110** (2013) 107007.

[56] Charnukha A. *et al.*, *Scientific Reports*, **5** (2015) 10392.

[57] Bussmann-Holder A. *et al.*, *Supercond. Nov. Magn.*, **30** (2017) 151-156

[58] Doria M. M., Cariglia M. and Perali A., *Physical Review B* , **94** (2016) 224513.

[59] Leggett A. J., *Modern Trends in the Theory of Condensed Matter,Lecture Notes in Physics*, Vol. **115**, edited by Pekalski A. and Przystawa R. (Springer-Verlag, Berlin) 1980

[60] Kugel K.I., Rakhmanov A.L., Sboychakov A.O., Poccia N. and Bianconi, A., *Phys. Rev. B*, **78** (2008) 165124.

[61] Bianconi A. *et al.* , *Supercond. Sci. Technol.*, **28** (2015) 024005.

[62] Campi *et al.*, *Nature*, **525** (2015) 359-362.

[63] Saini, N. L. *et al.*, *Eur. Phys. J. B*, **36** (2003) 75-80.

[64] Campi, G. *et al.* , *Eur. Phys. J. B*, **52** (2006) 15-21.